A measurement of $W b\bar{b}$ production and a search for monophoton signals of dark matter using the CMS detector at the CERN LHC

by

Thomas Mastrianni Perry

A dissertation submitted in partial fulfillment of
the requirements for the degree of

Doctor of Philosophy

(Physics)

at the

UNIVERSITY OF WISCONSIN–MADISON

2016

Date of final oral examination: 3 August 2016

The dissertation is approved by the following members of the Final Oral Committee:
Wesley Smith (Advisor), Professor, Physics
Sridhara Dasu, Professor, Physics
Matt Herndon, Professor, Physics
Yang Bai, Professor, Physics
David C. Schwartz, Professor, Chemistry

CONTENTS

LIST OF TABLES

LIST OF FIGURES

1 QUANTUM FIELD THEORY AND THE STANDARD MODEL

The Standard Model of particle physics (SM) is useful. It is a local Quantum Field Theory (QFT) representing the forefront of contemporary understanding of nature on its finest level and is simultaneously the most quantitatively verified physical model of the constituent elements of the universe and known to be an incomplete description. It is therefore one of the goals of modern society to experimentally investigate particles and the interactions between particles within the context of the SM to validate the theory where possible and to guide directions for its extension where necessary. To achieve this goal, the governments from nearly 100 different countries, states and territories have funded tens of thousands of scientists, engineers and technicians to build, operate, maintain and analyze data from the Large Hadron Collider (LHC) at the European Center for Nuclear Research (CERN). This thesis presents analyses of data taken with the Compact Muon Solenoid (CMS) detector using proton-proton collisions provided by the LHC during its operation in 2012 and 2015.

1.1 Local Quantum Field Theory

1.1.1 Representations of SU(2)

One of the key underlying principles behind any QFT is that of symmetry. In particular, QFTs arise from the combination of quantum mechanics with Lorentz symmetry which ensures that the equations used to describe the laws of physics remain equivalently valid in all inertial reference frames. Local fields are therefore required to transform as representations of the Lorentz group, namely rotations, J_a, and boosts, K_a where $a \in \{1, 2, 3\}$ for the three spatial dimensions. Boosts transform as vectors under rotation and the two obey the Lie algebras given in Equation 1.1, where ϵ_{abc} is the Levi-Civita symbol.

$$[J_a, J_b] = i\epsilon_{abc}J_c, \quad [K_a, K_b] = -i\epsilon_{abc}J_c, \quad [J_a, K_b] = i\epsilon_{abc}K_c \ . \tag{1.1}$$

Both J_a and K_a are hermitian, but it is natural to define the non-hermitian objects

$$L_a = \frac{1}{\sqrt{2}}\left(J_a + iK_a\right), \quad R_a = \frac{1}{\sqrt{2}}\left(J_a - iK_a\right) \tag{1.2}$$

which commute with each other and each independently obey the commutation relations of $SU(2)$,

$$[L_a, L_b] = i\epsilon_{abc}L_c, \quad [R_a, R_b] = i\epsilon_{abc}R_c, \quad [L_a, R_b] = 0 \ . \tag{1.3}$$

Table 1.1: *Selected representations of the Lorentz group are formed by combining representations of $SU(2)$ in the structure $SU(2)_L \times SU(2)_R$. The first column labels the quantum numbers, λ, and the second column translates this into dimensionality. The third column indicates the kind of object which meets the symmetry requirements.*

(λ_L, λ_R)	(d_L, d_R)		Name
$(0, 0)$	$(1, 1)$	ϕ	Scalar
$(1/2, 0)$	$(2, 1)$	ψ_L	Left-handed Weyl spinor
$(0, 1/2)$	$(1, 2)$	ψ_R	Right-handed Weyl spinor
$(1/2, 1/2)$	$(2, 2)$	A_μ	Gauge potential

Because of this, the Lorentz group may be expressed in terms of representations of $SU(2)_L \times SU(2)_R$.

The group $SU(2)$ can be thought of as the set of 2×2 complex matrices with unit determinant under the operation of matrix multiplication, and the $(2^2 - 1)$ generators of the group are proportional to the Pauli matrices,

$$\sigma_1 = \begin{pmatrix} 0 & 1 \\ 1 & 0 \end{pmatrix}, \quad \sigma_2 = \begin{pmatrix} 0 & -i \\ i & 0 \end{pmatrix}, \quad \sigma_3 = \begin{pmatrix} 1 & 0 \\ 0 & -1 \end{pmatrix} \tag{1.4}$$

which have been diagonalized along the 3 direction and combine with the unit matrix to form $\sigma^\mu = (\mathbf{1}, \vec{\sigma})$. Representations of $SU(2)$ are labelled by a quantum number, $\lambda \in \{0, 1/2, 1, 3/2, ...\}$, with the fundamental representation being $\lambda = 1/2$ and the dimensionality, d, of a representation being set by $d = 2\lambda + 1$. Representations of the full symmetry are therefore constructed by combining representations from the L and R components, and Table 1.1 illustrates those combinations of lowest dimensionality.

Rotations take spatial coordinates into spatial coordinates, but boosts mix spatial

coordinates with time, which have opposite signs in the spacetime metric. Therefore, under the parity operation, P, which inverts the signs of spatial coordinates,

$$P : J \to J, \quad P : K \to -K \ , \tag{1.5}$$

while, under conjugation, C, because J and K are hermitian,

$$C : J \to J, \quad C : K \to K \ . \tag{1.6}$$

Using Equation 1.2 then, the $(1/2, 0)$ and $(0, 1/2)$ representations transform as

$$P : \psi_{L(R)} \to \psi_{R(L)}, \quad C : \psi_{L(R)} \to \sigma_2 \psi^*_{R(L)}, \quad CP : \psi_{L(R)} \to \sigma_2 \psi^*_{L(R)} \ . \tag{1.7}$$

which illustrates the point that because ψ_L and ψ_R can be interchanged via these discrete transformations, they are not independent. The full $SU(2)_L \times SU(2)_R$ symmetry can thus be maintained by considering only one of the two, and it is customary to work with ψ_L, the 'left' component, henceforth simply denoted as ψ, with $\sigma_2 \psi^*_R$ denoted as $\overline{\psi}$. An object which transforms as a vector can be made from spinors by noting [1] that $(1/2, 0) \times (0, 1/2) = (1/2, 1/2)$. Therefore $\psi^\dagger \sigma^\mu \psi$ transforms as a Lorentz vector, and can be used to make a Lorentz-invariant object by contracting the spacetime index, μ. The derivative operator $\partial_\mu = (\partial/\partial t, \partial/\partial \vec{x})$ is translation-invariant and does not give a surface contribution if inserted between the two instances of ψ,

[1] $d = 2 \times 2(1/2) + 1 = 4$ for (t, x, y, z)

motivating the canonical kinetic term for spinors,

$$i\psi^\dagger\sigma^\mu\partial_\mu\psi \quad . \tag{1.8}$$

1.1.2 Yang-Mills Theory

The above construction for canonical kinetic terms in the Lagrangian was generalized by Chen Ning Yang and Robert Mills for N spinor fields as

$$i\sum_{a=1}^{N}\psi^{a\dagger}\sigma^\mu\partial_\mu\psi_a = i\Psi^\dagger\sigma^\mu\partial_\mu\Psi \quad , \tag{1.9}$$

and while the existence of this object is imposed by the Lorentz symmetry, further symmetries can be made apparent. A simple example is global phase invariance. For λ which is not a function of x, the transformation $\Psi \to e^{i\lambda}\Psi$ leaves the kinetic term in Equation 1.9 unchanged. The derivative passes through $e^{i\lambda}$ which combines with $e^{-i\lambda}$ from the transform on $\Psi^\dagger$ to make the unit.

A more complicated example is gauge invariance. The symmetry of global phase invariance can be extended by introducing (N^2-1) traceless hermitian matrices, $\boldsymbol{\lambda}_A$ which satisfy the Lie algebra,

$$[\boldsymbol{\lambda}_A, \boldsymbol{\lambda}_B] = if_{ABC}\boldsymbol{\lambda}_C, \quad \mathrm{Tr}\,(\boldsymbol{\lambda}_A\boldsymbol{\lambda}_B) = \frac{1}{2}\delta_{AB} \quad , \tag{1.10}$$

where f_{ABC} are the structure functions for $SU(N)$ and δ_{AB} is the Kronecker delta function. For $N=2$, $f_{ABC} = \epsilon_{abc}$ used in Equations 1.1 and $\boldsymbol{\lambda}_A$ are the Pauli matrices from Equations 1.4. For $N=3$, f_{ABC} is also a totally anti-symmetric operator and

$\boldsymbol{\lambda}_A$ are the Gell-Mann matrices.

These $\boldsymbol{\lambda}_A$ can each be used to construct a hermitian $(N \times N)$ matrix. One degree of freedom is factored out as the overall phase of the trace, demonstrated to be a symmetry of Ψ. This leaves $(N-1)$ degrees from the real diagonal elements and $2 \times {}^{(N^2-N)}/_2$ from the unique complex off-diagonal elements. These (N^2-1) overall degrees of freedom correspond to the $\boldsymbol{\lambda}_A$ which are used to construct

$$\mathbf{H} = \frac{1}{2} \sum_{A=1}^{N^2-1} \omega_A \boldsymbol{\lambda}_A \tag{1.11}$$

using ω_A as the parameter of expansion.

$\mathbf{H}$ can then be used to produce a unitary matrix

$$\boldsymbol{U} = e^{i\mathbf{H}} \tag{1.12}$$

whose unitarity is evident by the hermicity of $\mathbf{H}$. Unitarity is crucial for the final cancellation to leave Equation 1.9 invariant under the gauge transformation $\Psi \rightarrow \boldsymbol{U}\Psi$, but to ensure locality, the particular expansion, ω_a, could have dependence on position and thus interact with ∂_μ.

To accommodate for this, the derivative is generalized into an $(N \times N)$ covariant derivative matrix, $\boldsymbol{D}_\mu$, which has the property

$$\boldsymbol{D'}_\mu \boldsymbol{U}\Psi = \boldsymbol{U}\boldsymbol{D}_\mu\Psi \tag{1.13}$$

and thus behaves under gauge transformations as

$$\Psi \to \boldsymbol{U}\Psi, \quad \boldsymbol{D}_\mu \to \boldsymbol{D'}_\mu = \boldsymbol{U}\boldsymbol{D}_\mu\boldsymbol{U}^\dagger \quad . \tag{1.14}$$

Explicitly, $\boldsymbol{D}_\mu$ is constructed using (N^2-1) gauge potentials, A_μ, in the form of a hermitian matrix,

$$\mathbf{A}_\mu = \frac{1}{2}\sum_{B=1}^{N^2-1} A_\mu^B \boldsymbol{\lambda}_B \tag{1.15}$$

which transforms under gauge transformations as

$$\mathbf{A}_\mu \to \mathbf{A'}_\mu = -i\boldsymbol{U}\partial_\mu\boldsymbol{U}^\dagger - i\boldsymbol{U}\mathbf{A}_\mu\boldsymbol{U}^\dagger \quad . \tag{1.16}$$

The field strength matrix is formed by taking the commutator

$$\mathbf{F}_{\mu\nu} = -i[\boldsymbol{D}_\mu, \boldsymbol{D}_\nu] \tag{1.17}$$

which leads to a kinetic term that is invariant under both gauge and Lorentz transformations, $-1/2g^2\mathrm{Tr}\left(\mathbf{F}_{\mu\nu}\mathbf{F}^{\mu\nu}\right)$ where g is the coupling strength. This leads to the Yang-Mills Lagrange density of

$$\mathcal{L}_{\mathrm{YM}} = -\frac{1}{2}\mathrm{Tr}\left(\mathbf{F}_{\mu\nu}\mathbf{F}^{\mu\nu}\right) + i\Psi^\dagger\sigma^\mu\boldsymbol{D}_\mu\Psi + i\overline{\Psi}^\dagger\sigma^\mu\overline{\boldsymbol{D}}_\mu\overline{\Psi} \quad . \tag{1.18}$$

For $N = 2$, this is the Quantum ElectroDynamics (QED) Lagrangian of electromagnetic interactions with a massless electron, and for $N = 3$, this is Quantum ChromoDynamics (QCD).

1.2 The Standard Model

1.2.1 Gauge symmetry in $\mathbf{SU(3) \times SU(2) \times U(1)}$

The Standard Model (SM) Lagrangian uses the Yang-Mills construction on the group $SU(3) \times SU(2) \times U(1)$. Strong interactions are described by $SU(3)$ (color) which has eight gluons, G^A_μ, $A \in 1, 2, ..., 8$. Electroweak interactions incorporate the mixing of $SU(2) \times U(1)$ via the Higgs mechanism with $SU(2)$ (weak charge) having three weak bosons, W^a_μ, $a \in 1, 2, 3$ and $U(1)$ (hypercharge) having one hyperon B_μ. The field strengths are independent, with independent coupling constants g_3, g_2, g_1, each calculated using the appropriate covariant derivative in Equation 1.17. This is part of the SM Lagrangian describing the gauge bosons,

$$\mathcal{L}_{\text{bosons}} = -\frac{1}{4g_3^2} G^A_{\mu\nu} G^{\mu\nu A} - \frac{1}{4g_2^2} W^a_{\mu\nu} W^{\mu\nu a} - \frac{1}{4g_1^2} B_{\mu\nu} B^{\mu\nu} \quad . \tag{1.19}$$

The matter (antimatter) components are the spin-½ fermions which are built from the L representation of Weyl spinors and are listed in Table 1.2. The portion of the SM Lagrangian coming from the fermion kinetic terms is found by exchanging the derivative for the appropriate covariant derivative in Equation 1.9 to be

$$\mathcal{L}_{\text{fermions}} = i \sum_{i=1}^{3} \left(\mathbf{Q}_i^\dagger \sigma^\mu \boldsymbol{D}_\mu \mathbf{Q}_i + L_i^\dagger \sigma^\mu \boldsymbol{D}_\mu L_i + \overline{\mathbf{u}}_i^\dagger \sigma^\mu \boldsymbol{D}_\mu \overline{\mathbf{u}}_i + \overline{\mathbf{d}}_i^\dagger \sigma^\mu \boldsymbol{D}_\mu \overline{\mathbf{d}}_i \overline{e}_i^\dagger \sigma^\mu \boldsymbol{D}_\mu \overline{e}_i + \right) \tag{1.20}$$

with the covariant derivatives described in Table 1.3.

Both quarks and leptons come in three families, known as generations for the quarks and flavors for the leptons. The leptons are colorless and therefore do not

Table 1.2: *Fermions in the standard model consist of three families ($i \in 1, 2, 3$) of leptons and quarks in the singlet and doublet configurations. The symmetries are notated as $(SU(3)^c, SU(2))_Y$ where Y is chosen to satisfy the Gell-Mann-Nishijima formula, Equation 1.21.*

Name	Symbol	I_3	Symmetry
Quark doublet	$\mathbf{Q}_i = \begin{pmatrix} u_i \\ d_i \end{pmatrix}$	$\begin{pmatrix} 1/2 \\ -1/2 \end{pmatrix}$	$(3^c, 2)_{1/3}$
Lepton doublet	$L_i = \begin{pmatrix} \nu_i \\ e_i \end{pmatrix}$	$\begin{pmatrix} 1/2 \\ -1/2 \end{pmatrix}$	$(1^c, 2)_{-1}$
Quark singlet	$\overline{\mathbf{u}}_i$	0	$(3^c, 1)_{-4/3}$
Quark singlet	$\overline{\mathbf{d}}_i$	0	$(3^c, 1)_{2/3}$
Lepton singlet	$\overline{e}_i$	0	$(1^c, 2)_2$

Table 1.3: *The exact form of the covariant derivative used is determined by the couplings to gauge bosons the fermion has. Below, the fermions are listed, along with the associated derivative and interactions. On the bottom are the vectors of gauge potentials as defined in Equation 1.15.*

		Interactions		
Fermion type	Covariant derivative	$SU(3)$	$SU(2)$	$U(1)$
All quarks (doublet)	$\boldsymbol{D}_\mu \mathbf{Q}_i = \left(\partial_\mu + i\mathbf{G}_\mu + i\mathbf{W}_\mu + \frac{i}{3}B_\mu\right)\mathbf{Q}_i$	Yes	Yes	Yes
All leptons (doublet)	$\boldsymbol{D}_\mu L_i = \left(\partial_\mu + i\mathbf{W}_\mu + \frac{i}{2}B_\mu\right) L_i$	No	Yes	Yes
u-type quarks (singlet)	$\boldsymbol{D}_\mu \overline{\mathbf{u}}_i = \left(\partial_\mu - i\mathbf{G}^*_\mu - \frac{2i}{3}B_\mu\right)\overline{\mathbf{u}}_i$	Yes	No	Yes
d-type quarks (singlet)	$\boldsymbol{D}_\mu \overline{\mathbf{d}}_i = \left(\partial_\mu - i\mathbf{G}^*_\mu + \frac{i}{3}B_\mu\right)\overline{\mathbf{d}}_i$	Yes	No	Yes
Charged leptons (singlet)	$\boldsymbol{D}_\mu \overline{e}_i = \left(\partial_\mu + iB_\mu\right)\overline{e}_i$	No	No	Yes

$\mathbf{G}_\mu = G^A_\mu \boldsymbol{\lambda}^A/2, \quad \mathbf{G}^*_\mu = G^A_\mu \boldsymbol{\lambda}^{A*}/2, \quad \mathbf{W}_\mu = W^a_\mu \boldsymbol{\sigma}^a/2$

couple to gluons, but the quarks do and additionally come in three color varieties for each generation. The singlet configurations contain only electrically charged fermions,

and all fermions have their charge set by the Gell-Mann-Nishijima formula,

$$Q = I_3 + \frac{Y}{2} \quad , \tag{1.21}$$

where I_3 is the component of weak isospin, $SU(2)$, along the direction in which the Pauli matrices in Equations 1.4 are diagonalized.

All quarks and leptons can exist in $SU(2)$ doublet configurations, and the different I_3 values further break quarks and leptons into types. For quarks, there are u-type (u, c, t) = (up, charm, top) which have charge $+2/3$, and there are d-type (d, s, b) = (down, strange, bottom) which have charge $-1/3$. Leptons are either charged (e, μ, τ) = (electron, muon, tauon) or neutral $(\nu_e, \nu_\mu, \nu_\tau)$ = (electron-, mu-, tau-neutrino), and all charged fermions are arranged such that mass increases with successive generations within a given type. In units where $\hbar = c = 1$, the top ($m_t = 173$ GeV) and bottom ($m_b = 4$ GeV) are the heaviest quarks of their respective types, with the bottom weighing three orders of magnitude greater than the lightest quark, up ($m_u = 2$ MeV). The mass separation for the charged leptons ($m_\tau = 1.7$ GeV, $m_e = 0.5$ MeV) also spans multiple orders of magnitude, but while the observations of neutrino oscillations indicate that neutrinos have mass, only upper limits on the values they may have have been set on the order of MeV.

1.2.2 Symmetry breaking in $\mathbf{SU(2) \times U(1) \rightarrow U(1)}$

Fermions and gauge bosons are massless as written in $\mathcal{L}_{\text{fermions}}$ and $\mathcal{L}_{\text{bosons}}$, but are observed to be massive in nature and can acquire mass through the Brout-Englert-

Higgs mechanism. A scalar (spin-zero) field as given in the top row of Table 1.1 is introduced in a doublet configuration. This adds a Higgs term to the SM Lagrangian,

$$\mathcal{L}_{\text{Higgs}} = \left(\boldsymbol{D}_\mu H\right)^\dagger \boldsymbol{D}_\mu H + m_H H^\dagger H - \lambda \left(H^\dagger H\right)^2 \quad , \tag{1.22}$$

where the first term is the canonical kinetic term for a scalar, the second term generates the mass of the Higgs boson (m_H) and the third term is a potential. This is minimized when

$$H_0^\dagger H_0 = \frac{m^2}{2\lambda} = \frac{v^2}{2}, \quad H_0 = \frac{1}{\sqrt{2}} \begin{pmatrix} 0 \\ v \end{pmatrix} \quad . \tag{1.23}$$

Taking perturbations about the minimum vacuum expectation value using the Kibble parameterization, $v \to v + h(x)$ and the unitary matrix containing three Nambu-Goldstone bosons from the symmetry breaking is factored out, yielding

$$H = \frac{1}{\sqrt{2}} \boldsymbol{U}(x) \begin{pmatrix} 0 \\ v + h(x) \end{pmatrix} \quad . \tag{1.24}$$

In this gauge, the weak bosons, $W^a_{\mu\nu}$, and the hyperion, B_μ appear in Equation 1.25 as linear combinations as the massive $W^\pm$ and Z bosons, and as the massless photon respectively,

$$\begin{gathered} W^\pm_\mu = \tfrac{1}{\sqrt{2}} \left(W^1_\mu \mp i W^2_\mu\right), \quad Z_\mu = \cos\theta_W W^3_\mu - \sin\theta_W B_\mu, \quad A_\mu = \sin\theta_W W^3_\mu + \cos\theta_W B_\mu \\ M_Z = \tfrac{v}{2}\sqrt{g_1^2 + g_2^2}, \quad M_W = \cos\theta_W M_Z \quad . \end{gathered} \tag{1.25}$$

Here, the Weinberg angle, $\theta_W = {}^{g_1}/_{g_2}$, is the ratio between the $U(1)$ and $SU(2)$. The $\pm$ in $W^{\pm}_{\mu}$ aligns with the electric charge of the W boson, and the Z_μ and A_μ are both electrically neutral and orthogonal.

The vector boson couplings to the fermions are then expressed as three types of currents. Electromagnetic interactions, J^{γ}_{μ}, involve couplings between the photon, γ, and charged particles, and any particle which interacts with the photon can also interact with the Z boson. The neutral current interactions, J^{Z}_{μ}, have additional couplings to the lepton and quark doublets and the charged current interactions, $J^{\pm}_{\mu}$, are between the doublets and the W bosons. Couplings to each of the bosons are scaled by a coupling factor which decides the relative strengths of the interactions, and the Lagrangian for the currents is given in Equation 1.26 where i indicates the generation.

$$
\begin{aligned}
\mathcal{L}_{\text{currents}} &= eA^{\mu}J^{\gamma}_{\mu} + g_Z Z^{\mu}J^{Z}_{\mu} + g_W W^{+\mu}J^{-}_{\mu} + G_W W^{-\mu}J^{+}_{\mu} \\
J^{\gamma}_{\mu} = \;& \bar{e}^{\dagger}_i\sigma_\mu\bar{e}_i + e^{\dagger}_i\sigma_\mu e_i + \tfrac{2}{3}\mathbf{Q}^{\dagger}_{i1}\sigma_\mu\mathbf{Q}_{i1} - \tfrac{1}{3}\mathbf{Q}^{\dagger}_{i2}\sigma_\mu\mathbf{Q}_{i2} - \tfrac{2}{3}\overline{\mathbf{u}^{\dagger}_i}\sigma_\mu\overline{\mathbf{u}_i} + \tfrac{1}{3}\overline{\mathbf{d}^{\dagger}_i}\sigma_\mu\overline{\mathbf{d}_i} \\
J^{\mathrm{Z}}_{\mu} = \;& L^{\dagger}_i\tfrac{\tau_3}{2}\sigma_\mu L_i + \mathbf{Q}^{\dagger}_i\tfrac{\tau_3}{2}\sigma_\mu\mathbf{Q}_i - \sin^2\theta_W J^{\gamma}_{\mu} \\
J^{\pm}_{\mu} = \;& L^{\dagger}_i\tau_{\pm}\sigma_\mu L_i + \mathbf{Q}^{\dagger}_i\tau_{\pm}\sigma_\mu\mathbf{Q}_i \\
& e = \tfrac{g_1 g_2}{\sqrt{g_1^2+g_2^2}}, \quad g_Z = \tfrac{e}{\cos\theta_W\sin\theta_W}, \quad g_W = \tfrac{e}{\sqrt{2}\sin\theta_W}
\end{aligned}
\tag{1.26}
$$

1.2.3 Yukawa couplings and the CKM matrix

In addition to generating mass terms for the bosons, the Higgs field gives rise to fermion mass via Yukawa couplings between the Higgs doublet, H, from Equation 1.22 and the fermion doublets. A singlet configuration is possible to construct from

two $SU(2)$ doublets in their antisymmetric combination[2], of the general form (MN) where M and N are both L fermion fields. Each term has an associated Yukawa coupling, $\mathbf{Y}^f = y_{ij}$, where $f \in \{u, d, e\}$ for each of the charged fermion types, and this piece of the SM the Lagrangian is

$$\begin{aligned} \mathcal{L}_{\text{Yukakwa}} &= y^u_{ij}\mathbf{Q}_i\overline{\mathbf{u}}_j H + y^d_{ij}\mathbf{Q}_i\overline{\mathbf{d}}_j\overline{H} + y^e_{ij}L_i\overline{e}_j\overline{H} \\ &= \mathcal{L}^u_{\text{Yuk}} + \mathcal{L}^d_{\text{Yuk}} + \mathcal{L}^e_{\text{Yuk}} \end{aligned} \quad . \tag{1.27}$$

In general, any (3×3) matrix can written in terms of a diagonal matrix D and two unitary matrices U and V, and in particular, the coupling matrices can be expressed as $\mathbf{Y^f} = \mathbf{U}^f\mathbf{D}^f\mathbf{V}^f$. The fermion Yukawa couplings are all of the form $\mathbf{Y}^f\mathbf{F}\overline{\mathbf{f}}$ and by incorporating $\mathbf{V}^f$ into $\overline{\mathbf{f}}$, the may each be individually diagonalized as

$$\begin{aligned} \mathcal{L}^e_{\text{Yuk}} &= \Big(m_e(\overline{e}e) + m_\mu(\overline{\mu}\mu) + m_\tau(\overline{\tau}\tau)\Big)\,\beta(h) \\ \mathcal{L}^d_{\text{Yuk}} &= \Big(m_d(\overline{d}d) + m_\mu(\overline{s}s) + m_\tau(\overline{b}b)\Big)\,\beta(h) \\ \mathcal{L}^u_{\text{Yuk}} &= \Big(m_u(\overline{u}u) + m_\mu(\overline{c}c) + m_\tau(\overline{t}t)\Big)\,\beta(h) \end{aligned} \tag{1.28}$$

where β is a function of the Higgs coupling, h. The mass terms for the gauge bosons are also proportional to h. It is because the mass of the Higgs boson is tied to the masses of the gauge bosons and charged fermions that the discovery of the Higgs boson in 2012 was of such importance. The result was announced just a few months after I moved to Geneva to do research at CERN, and it provided the first measurement of a parameter in the SM that had been previously unknown, $m_H = 125\text{GeV}$.

Unlike the leptons, which contain only one charged type, the quarks have two

[2] The second term in $(1/2, 0) \times (1/2, 0) = (1, 0) + (0, 0)$

different spinor fields, **u** and **d**, which are different but both have Yukawa couplings to the Higgs with the same **Q**. This means that while the lepton sector $\mathcal{L}^{e}_{\text{Yuk}}$ can be diagonalized in mass simultaneously with either of $\mathcal{L}^{d}_{\text{Yuk}}$ or $\mathcal{L}^{u}_{\text{Yuk}}$, the quarks can not be simultaneously diagonalized. The mismatch between the two types of quarks is characterized by the unitary Cabibbo-Kobayashi-Maskawa (CKM) matrix,

$$\mathcal{U}_{\text{CKM}} = \mathbf{U}^{d}\overline{\mathbf{U}}^{u\dagger} = \begin{pmatrix} c_1 & +s_1c_3 & +s_1s_3 \\ -s_1c_2 & c_1c_2c_3 - s_2s_3e^{i\delta} & c_1c_2s_3 + s_2c_3e^{i\delta} \\ -s_1s_2 & c_1s_2c_3 + c_2s_3e^{i\delta} & c_1s_2s_3 - c_2c_3e^{i\delta} \end{pmatrix} \tag{1.29}$$

where s_a and c_a stand for $\sin\theta_a$ and $\cos\theta_a$. In this choice of basis, the charged current interactions from Equation 1.26 are

$$J^{\pm}_{\mu} = L^{\dagger}_{i}\tau_{\pm}\sigma_{\mu}L_i + \mathbf{d}^{\dagger}_{i}\left(\mathcal{U}_{\text{CKM}}\right)_{ij}\tau_{\pm}\sigma_{\mu}\mathbf{u}_j \quad . \tag{1.30}$$

The CKM matrix thus is a matrix of coefficients for transforming between generations and types of quarks for charged current interactions. It also is the location in the SM where parity invariance is violated.

The laws of nature are postulated to be invariant under the combined operation CPT, where C and P are defined in Equations 1.5 and 1.6, and T is the antiunitary time-reversal operator,

$$T^{-1}iT = -i \tag{1.31}$$

Because of the complex phase, δ, in the CKM matrix, the couplings between the quarks and W bosons are not T invariant. To maintain CPT invariance, $\delta \neq 0$

implies that CP must be violated in such interactions.

1.3 Interpreting the Standard Model

1.3.1 Scattering amplitude and propagators

Initial and final states are built by successive applications of the raising (or particle creation) operator, $a^\dagger$, on the vacuum, $|0\rangle$, at the limit of initial states being measured infinitely far in the past and final states being measured infinitely far in the future.

$$|i\rangle = \lim_{t\to-\infty} \sum_i a_i^\dagger |0\rangle, \quad |f\rangle = \lim_{t\to+\infty} \sum_{i'} a_{i'}^\dagger |0\rangle \tag{1.32}$$

The overlap or scattering amplitude between these states, $\langle f|i\rangle$, can be expressed using the Lehmann-Symanzik-Zimmermann (LSZ) reduction formula in Equation 1.33 as factored into two pieces,

$$\langle f|i\rangle = i^{n_j+n_{j'}} \int \prod_{\mathrm{j}} d^4x_{\mathrm{j}} e^{ik_{\mathrm{j}}x_{\mathrm{j}}} \left(-\partial_{\mathrm{j}}^2 + m^2\right) \times \langle 0|\mathrm{T} \prod_{\mathrm{j}} \phi(x_{\mathrm{j}})|0\rangle \tag{1.33}$$

The first piece is made of integrals over the momenta, k_{j} for $\mathrm{j} \in j, j'$, of the n_j incoming and $n_{j'}$ outgoing particles. In these integrals, each plane wave multiplies the function $(-\partial_j^2 + m^2)$ where $\partial_{\mathrm{j}}^2 = \partial_{\mathrm{j}}^\mu \partial_{\mu\mathrm{j}}$ is the contraction of the Lorentz-invariant derivative operator. The second piece of the LSZ formula is the vacuum expectation value of the time-ordered product of fields, $\langle 0|\mathrm{T} \prod_{\mathrm{j}} \phi(x_{\mathrm{j}})|0\rangle$.

By Wick's theorem, the time-ordered interaction of n fields is identically zero for

odd numbers of fields, and for even numbers of fields is

$$\langle 0|\mathrm{T}\phi(x_1)\dots\phi_(x_{2n})|0\rangle = \frac{1}{i^n}\sum_{\text{pairs}}\Delta(x_{i1}-x_{i2})\dots\Delta(x_{i_{2n-1}}-x_{i_{2n}}). \tag{1.34}$$

In this equivalence, $\Delta(x-x')$ is the Feynman propagator between x and x' and is Green's function for the Klein-Gordan equation which contains the same $(-\partial_{\mathrm{j}}^2+m^2)$ term as multiplies in the integrals,

$$\left(-\partial_x^2+m^2\right)\Delta(x-x') = \delta^4(x-x') \quad . \tag{1.35}$$

In this way the two components of the LSZ formulation interact. The integrals contain factors of $(-\partial^2+m^2)$ and the propagators contain factors of $1/(-\partial^2+m^2)$. The on-shell requirement, that $|f\rangle$ and $|i\rangle$ have fixed masses causes $(-\partial^2+m^2)\to 0$. This term in the integral cancels exactly with the corresponding diverging term in the appropriate propagator, but sets to zero the terms which do not have this divergence. This is the mechanism by which final state particles are observed to be on their mass shell, or on-shell, while allowing for interactions to happen between particles at varying masses, off-shell, with varying probabilities.

1.3.2 Path integrals and Feynman diagrams

To calculate the expression in 1.34, an integral over paths through the space of field configurations is used. This is called the path integral, $Z(J)$, and is a function of the

Lagrangian, $\mathcal{L}$, current sources, J, and fields, ϕ,

$$Z(J) = \langle 0|0\rangle_J = \int \mathcal{D}\phi \; e^{i\int d^4x(\mathcal{L}+J\phi)} \quad . \tag{1.36}$$

The fundamental interactions between particles as described by $Z(J)$ can be visually represented using the Feynman diagram notation. On a 2-D spacetime plane, (x,t), lines representing particles meet at a vertex, which is the interaction point. Fermions are represented using solid lines with an arrow indicating a direction. If the component of the arrow in the t dimension is positive, the particle fermion is indicated, and if it is negative, the antiparticle is meant. In this way, by rotating $(x,t) \to (x',t')$ a single diagram can be interpreted as depicting possibly more than one interaction.

To describe the scattering of fermions and gauge bosons in the SM, diagrams with the appropriate initial and final state particles are constructed from the vertices illustrated in Figure 1.1. Three-point vertices are made from the intersection of three line segments at a point, and four-point vertices are made from the intersection of four line segments. External lines correspond to real particles which are observed in the final state and are on-shell. Internal lines correspond to virtual particles that not observed in the final state and therefore may or may not be on-shell.

A diagram is tree-level if it uses the smallest number of vertices possible to depict an interaction having the correct initial and final states. For the case of two fermions, $\phi(x_1), \phi(x_2)$, which scatter via a gauge boson that subsequently decays to two possibly different fermions, $\phi(x_1'), \phi(x_2')$, the three unique tree-level diagrams for a given configuration of $\phi(x_1), \phi(x_2), \phi(x_1'), \phi(x_2')$, are illustrated in Figure 1.2.

These specific diagrams are depictions of the s, t, u channels respectively, named after the Mandelstam variables, which are Lorentz scalar combinations of incoming and outgoing momenta,

$$\begin{aligned} s = &\quad -(k_1 + k_2)^2 = \quad -(k_1' + k_2')^2 \quad , \\ t = &\quad -(k_1 + k_1')^2 = \quad -(k_2' - k_2')^2 \quad , \\ u = &\quad -(k_1 + k_2')^2 = \quad -(k_2 - k_1')^2 \quad . \end{aligned} \tag{1.37}$$

The Mandelstam variable s is the square of the momenta of the incoming particles in the center-of-mass (CM) frame and $\sqrt{s}$ is the typical variable used by experimentalists to discuss the energy of colliding beams of particles.

Combining contributions from all valid Feynman diagrams according to the stastical rules appropriate for the particles which participate in the interaction, gives $W(J)$ where

$$Z(J) = e^{iW(J)} \tag{1.38}$$

and the time ordered product of the fields can be found by taking the appropriate functional derivatives on W,

$$\langle 0|\mathrm{T}\phi(x_1)\ldots\phi(x_N)|0\rangle = \delta_1 \ldots \delta_N iW(J)|_{J=0} \quad . \tag{1.39}$$

1.3.3 Renormalization

Crucial for the LSZ formulation are two features of quantum fields, that they are fully separable in the infinite limit, $\langle 0|\phi(x)|0\rangle = 0$, and that they are states of definite

Figure 1.1: *The couplings for the SM gauge interactions.*

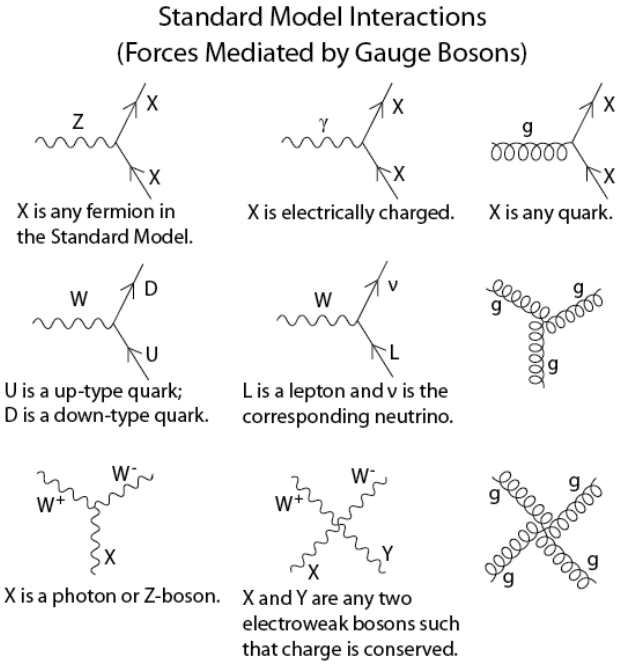

Figure 1.2: *Below are Feynman diagrams for* $2 \to 2$ *scattering. These are the tree-level diagrams of the* s, t, u *channels respectively.*

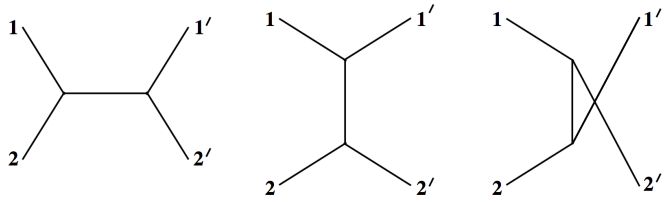

momentum, $\langle k|\phi(x)|0\rangle = e^{-ikx}$. In the SM, which allows for fields to interact, these conditions are guaranteed by adjusting the strengths of the fundamental couplings, g_1, g_2, g_3. This ensures that the quantum states remain properly normalized, and is thus called renormalization.

Renormalization is necessary to account for corrections to the tree-level propagators

Figure 1.3: *Renormalization takes place via a modification of the coupling parameters g_1, g_2, g_3 to account for the contributions that loops of virtual particles make on the propagators and vertices. Below are diagrams keeping track of the flow of momentum for one-loop corrections to the propagator and three and four point vertices.*

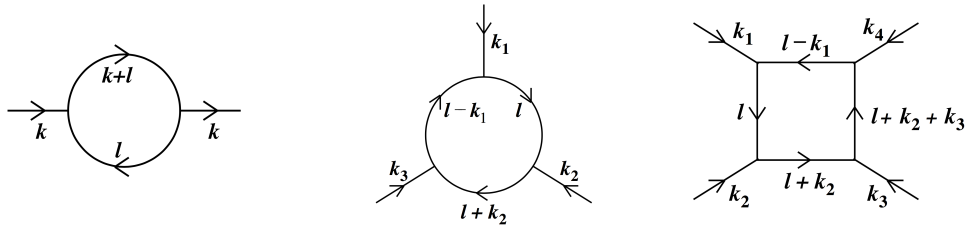

and vertices which arise from contributions of virtual particles connecting to form closed internal loops. The lowest order, one-loop, diagrams are illustrated in Figure 1.3. Renormalization is accomplished by introducing an energy scale, and assuming that the couplings are small compared this this scale. The coupling constants are therefore functions of energy and are quoted at a particular renormalization scale, μ_R.

1.3.4 Cross sections and decay rates

The scattering amplitude $\langle f|i\rangle$ is not a directly measurable observable. What can be observed is some finite distribution of data which may be analyzed to reveal information about the scattering amplitude. Quantum mechanics dictates that only predictions of probability are possible, and the final probability of observing a particular interaction is dependent on many variables, including the energies, types and angular momenta of the incoming and outgoing particles as well as the masses of the propagators and the orientation and efficiency of the detector.

A quantity typically measured is therefore the interaction cross section, σ, and

for the scattering of two incoming particles going to n' particles, $2 \to n'$, in the CM frame, the differential is

$$d\sigma = \frac{1}{4|\mathbf{k}_1|_{\mathrm{CM}}} |\mathcal{T}|^2 \, d\mathrm{LIPS}_{n'}(k_1 + k_2) \tag{1.40}$$

where the scattering matrix element, $\mathcal{T}$, is defined using Equation 1.33, as

$$\langle f|i\rangle = (2\pi)^4 \delta^4 \left(\sum k_{\mathrm{in}} - \sum k_{\mathrm{out}} \right) i\mathcal{T} \tag{1.41}$$

and the Lorentz-invariant measure of the phase space for the n' outgoing particles is

$$d\mathrm{LIPS}_{n'}(k) = (2\pi)^4 \delta^4 \left(k - \sum_{j=1}^{n'} k'_i \right) \prod_{j=1}^{n'} dq'_j \tag{1.42}$$

with the Lorentz-invariant differential dq.

The cross section is used to calculate the rate at which a process occurs, but is not the only relevant factor in determining the overall production rate. The production rate of a given final state is also dependent on the incoming rate of possible interactions and is known as luminosity, $\mathcal{L}$. Luminosity has the units of inverse area per unit time and the total number of events produced is therefore proportional to $\int \mathcal{L} dt$. In any real detector, final state particles are collected only within a finite solid angle and the number of particles scattered into a given solid angle, Ω, is given by

$$\frac{dN}{d\Omega} = \mathcal{L} \frac{d\sigma}{d\Omega} \quad . \tag{1.43}$$

It is also possible for particles to decay as $1 \to n'$. Massive particles decay to

lighter ones in both the fermion and boson sectors, with all massive bosons able to spontaneously decay via the diagrams in Figure 1.1. Of the charged fermions, only the first generation is stable for each type, and neutrinos are not known to spontaneously decay, but oscillate between flavors while propagating in free space. Like the differential cross section, the differential decay rate is a function of the scattering amplitude and has integration measure $d\text{LIPS}$,

$$d\Gamma = \frac{1}{2E}|\mathcal{T}|^2 \, d\text{LIPS}_{n'}(k) \quad . \tag{1.44}$$

The differential decay rate is inversely proportional to the energy of the particle, $E = \sqrt{m^2 + p^2}$. This means that comparitively heavy particles will decay faster than comparitively light ones and that energetic particles will appear to live longer for a stationary observer due to relativistic time dilation effects. The total decay rate of a given particle is found by summing the decay rates from each of the contributing processes, and the primary decay channels and rates for the fundamental particles are given in Table 1.4.

At CMS, the heaviest quark and the heaviest lepton both decay before reaching the detector volume. This makes b quarks the heaviest fundamental particles which can be seen to decay inside the detector, and therefore an object of interest. Additionally, their heavy mass means that they couple strongly with the Higgs boson which still has many properties that are under investigation. The W and Z bosons are both so massive that they decay before reaching the innermost layers of the detector and are often identified by their decay products pointing back to a common vertex.

Table 1.4: *Below are listed the decay channels and rates for each of the unstable fundamental particles. At CMS, with the detection apparatus located a finite distance away from the interaction vertex, particles such as the W, Z and Higgs bosons, as well as the t and tau, decay before reaching the first layer of the detector.*

Particle	Primary decay modes(s)	Total rest-frame $d\Gamma$	Typical decay location
W	$W \to \ell\nu$	X	Before reaching CMS
Z	$Z \to f\overline{f}$ (for $2M_f < M_Z$)	X	Before reaching CMS
τ	$\tau \to W\nu_\tau$	X	Before reaching CMS
μ	$\mu \to W\nu_\mu$	X	After leaving CMS
t	$t \to W^+b$	X	Before reaching CMS
b	$b \to W^-c$	X	Inside CMS
c	$c \to W^+s$	X	Inside CMS
s	$s \to W^-u$	X	Inside CMS

1.3.5 QCD and Proton Structure

The Feynman diagrams introduced in Section 1.3.2 describe the interactions between fundamental particles, but at the LHC, collisions take place between protons, which are composit.

One feature of the $SU(3)$ symmetry of the strong force is that gluons carry one unit of color and one unit of anticolor while the quarks carry one unit of color charge. This is what allows gluons to interact with each other as well as with quarks. That quark confinement is necessitated by the $SU(3)$ structure has not been conclusively determined, but observationally, a free gluon or quark has never been observed. Instead, quarks appear as bound in colorless (singlet) combinations called hadrons which are further classified as mesons ($q\overline{q}$) or as baryons (qqq or $\overline{qqq}$), and are held together by gluons. Evidently, the binding energy of the quarks has a form such

that after a distance of roughly 10^{-15} meters, the energy stored in the gluon field is greater than the energy needed to create a quark-antiquark pair, bringing the pair into existance. This process of energetic quarks creating particles as they separate is called hadronization and is an important effect at the LHC.

Protons are a type of baryon and at low energy, may combine with a single electron to form a neutral hydrogen atom. At higher energies, the internal structure of the proton becomes more evident, and it contains three valence quarks, uud, which are constantly exchanging gluons. When probed at high enough energy, or equivalently, at short enough length scales, these gluons can also each split into a $q\bar{q}$ pair which typically reannihialate with each other. With gluons inside the proton splitting into quarks and coupling with other gluons, this forms a 'sea' of quarks and gluons, and as protons are acceleratded to energies of GeV or TeV as is the case at the LHC, the fraction of the momentum of the proton attributed to the gluons becomes higher than that attributed to the valence quarks.

A proton-proton collider was therefore a sensible choice for the LHC. The physics goals of the project are to measure quantities associated with a wide range SM processes and to continue the search for evidence of new physics. Quarks interact with all of the gauge bosons as well as with the Higgs boson and the proton contains the two lightest quarks of each type in addition to the gluons and sea. Colliding proton beams thus allow for the interactions between many different initial particle configurations to be explored, and with the exception of the neutrinos which interact only via the weak exchange of the Z boson and escape the detectors, all other fundamental SM particles have been directly observed at CERN.

2 PHENOMENOLOGY OF PROCESSES

2.1 The process $pp \to W b\bar{b} \to \ell\nu b\bar{b}$

Figure 2.1: *The Feynman diagram for the process $pp \to W b\bar{b} \to \ell\nu b\bar{b}$ is illustrated below, and is composed from the individual vertices illustrated on the left, each of which is described in Section 2.1.*

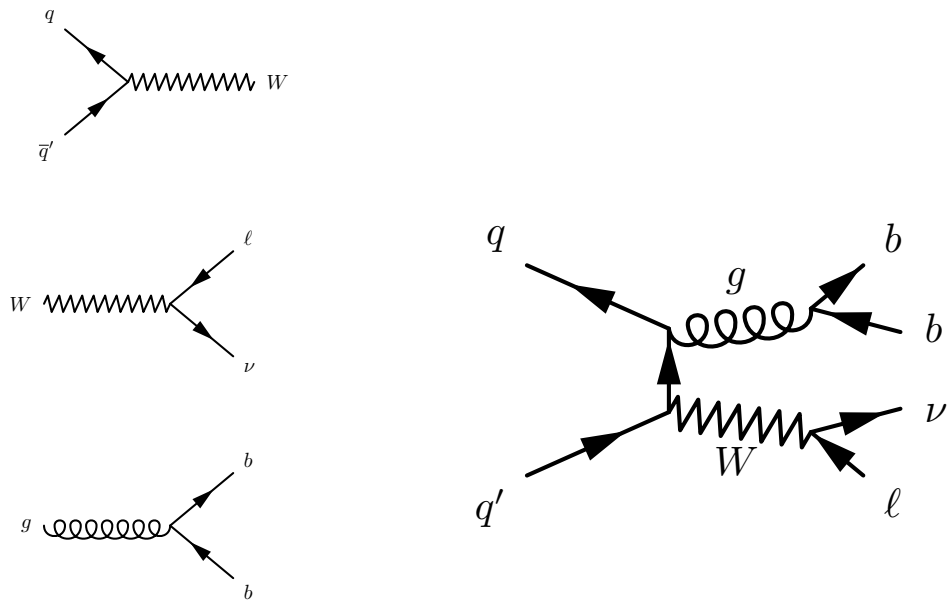

2.1.1 $pp \to W$

The W boson couples to all charged fermions and can be created during the collision of a quark-antiquark pair with a relative charge difference of e. In the proton are quarks and the most prevalant valence quark is the u. Therefore in a pp collision, the channel by which most W bosons are produced is via a the annihilation of a valence

u quark from one proton with a $\overline{d}$ from the sea of the other, $u\overline{d} \to W^+$. Quarks of higher generation can also be found inside the sea as the result of gluons splitting into $q\overline{q}$ pairs, but all interactions are modified by a coefficient in the CKM matrix and higher generation mixing is thus suppressed. In this thesis, all modes of $pp \to W^{\pm}$ production are considered.

2.1.2 $W \to \ell\nu$

Just as the W boson can be created by the collision $q\overline{q}' \to W$, it can also decay as $W \to q\overline{q}'$. This is known as hadronic W decay and can be a useful analysis channel for experimentalists, especially for decay products with energies approaching the TeV scale. Leptonic W decay, $W \to \ell\nu$, is also an important channel for experimentalists and is the one considered in this analysis. Because leptons constitute a negligible fraction of the sea, the detection of leptons at high energy after a pp collision is often a good indicator of the decay of a massive gauge boson, $W \to \ell\nu$ or $Z \to \ell\overline{\ell}$.

The W boson is much heavier than any of the leptons and therefore decays with roughly equal probability to any of $e\nu_e, \mu\nu_\mu, \tau\nu_\tau$. From Table 1.4, tauons created at CMS subsequently decay before reaching the detector, so for this analysis, the decay channel of the W investigated is $W \to \ell\nu$ where $\ell \in e, \mu$.

2.1.3 $g \to b\overline{b}$

Because quarks couple strongly to gluons and $q\overline{q}' \to W$ has been shown to be an important production channel in pp collisions, it is possible for one of the initial state quarks to radiate a gluon. This is called initial state radiation, ISR, and if the gluon

is produced with enough energy, it is capable of splitting to a quark-antiquark pair. In particular, a $g \to b\bar{b}$ vertex can be added to either of the incoming quarks.

2.2 The process $pp \to \mathrm{Z}\gamma \to \nu\bar{\nu}\gamma$

Figure 2.2: *The Feynman diagram for the process $pp \to \mathrm{Z}\gamma \to \nu\bar{\nu}\gamma$ is illustrated below, and is composed from the diagrams illustrated on the left, each of which is described in Section 2.2.*

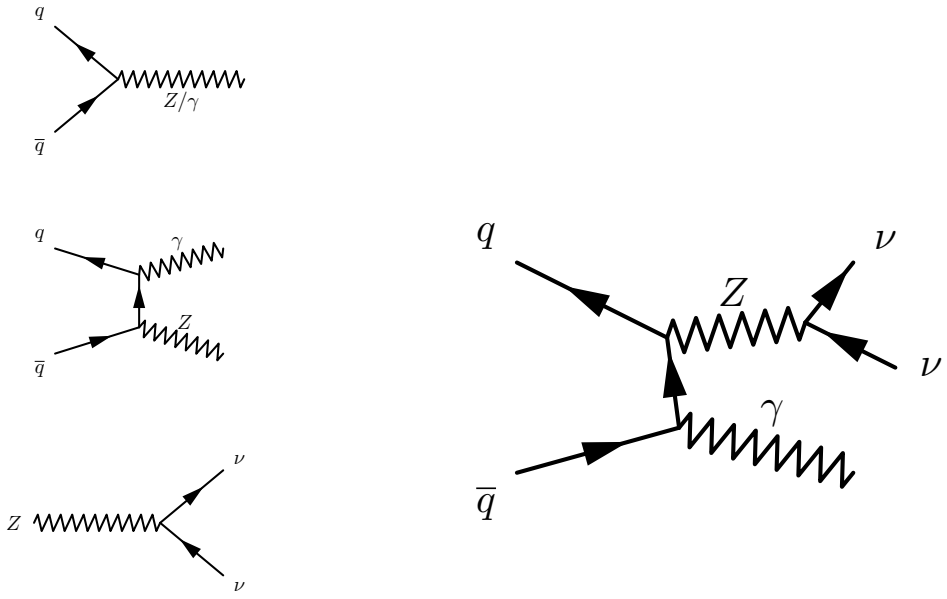

2.2.1 $pp \to \mathrm{Z}/\gamma$

Similar to the W boson, the Z boson and the photon can also each be produced via the collision of quarks in the process $q\bar{q} \to Z/\gamma$. Unlike interactions with the W boson, interactions with Z/γ conserve parity invariance and do not transport charge.

Any interaction which can happen as mediated by a photon can also happen with the exchange of a Z boson, but for collisions at $\sqrt{s} < M_Z = 90$ GeV, the Z can not be made on-shell. In this low energy regime γ exchange dominates, but in 2015, the LHC ran at $\sqrt{s} = 13$ TeV and the relative mass difference between the Z and the γ played a negligible role in their relative rates of production.

2.2.2 $pp \rightarrow \mathrm{Z}\gamma$

2.2.3 $\mathrm{Z} \rightarrow \nu\overline{\nu}$